LncRNA TSIX acts as a ceRNA of miR-342-3p to Promote the Progression of Nasopharyngeal Carcinoma by Regulating AGR2

Shupeng Chen
Jinan University
Qiongxia Zhang
Jinan University
Zhenyu Li
Jinan University
Xintian Qin
Guangdong Pharmaceutical University
Zhe Wang
Guangdong Pharmaceutical University
Huimin Liu
Guangdong Pharmaceutical University
Kailan Mo
Guangdong Pharmaceutical University
Shaoyun Wu
Sun Yat-Sen University
Yaoying Li
Sun Yat-sen University Cancer Center
Dan Wang
Sun Yat-sen University Cancer Center
Zhi Shi
Jinan University
Xingxiang He (XingxiangHeWest@163.com)
Jinan University

Research article

Keywords: NPC, TSIX, MiR-342-3p, AGR2, Apoptosis

Posted Date: December 21st, 2020

DOI: https://doi.org/10.21203/rs.3.rs-58760/v1

Abstract

Background: LncRNA TSIX has been observed to be abnormally expressed in many human cancers. However, its roles in nasopharyngeal carcinoma (NPC) remains unclear, and this study aims to explore the functions of TSIX in NPC.

Methods: The expression of TSIX and miR-342-3p in NPC tissues and corresponding cell lines was detected by qRT-PCR. Bioinformatics analysis and luciferase activity assay and RIP assay were applied to determine the interaction between TSIX, miR-342-3p, and AGR2. The roles of TSIX, miR-342-3p and AGR2 in the proliferation, apoptosis, migration and invasion of NPC cells were explored both *in vitro* and *in vivo*. In addition, the rescue experiments were used to confirm the functions of TSIX, miR-342-3p, and AGR2 in NPC progression.

Results: Our study firstly found that TSIX was significantly upregulated in NPC tissues and corresponding cell lines. Moreover, upregulation of TSIX obviously exacerbated the NPC progression including the proliferation, apoptosis, migration and invasion, while downregulation of TSIX efficiently attenuated the development of NPC. Further, our results demonstrated that TSIX could increase the expression of AGR2, which was directly targeted by miR-342-3p, and then lead to the facilitated development of NPC cells.

Conclusion: In summary, our study revealed that lncRNA TSIX promoted the progression of NPC through targeting miR-342-3p/AGR2 axis, suggested that it might be a potential therapeutic target for NPC.

Background

Nasopharyngeal carcinoma (NPC) is an umbrella term for a group of malignant epithelial tumors, and some of which have a dramatically skewed geographical and ethnic distribution and exhibits virtually 100% association with Epstein Barr virus(1). Although NPC is uncommon in the United States with only 0.2 to 0.5 cases per 100,00 people, the incidence is 25 to 50 per 100,000 people in southern China and Hong Kong(2). Epidemiological trends of previous studies have shown that its incidence has declined gradually but progressively and mortality has been reduced substantially(3). Moreover, the prognosis of NPC patients has improved significantly over the past three decades due to advances in disease management, diagnostic imaging, radiotherapy technology, and broader application of systemic therapy(4). Hence, the study of molecular mechanisms in NPC is still urgent and may help to identify efficient therapeutic and diagnostic targets(5–7).

Long non-coding RNAs (lncRNAs) are a class of non-protein coding RNAs with approximately with greater than 200 nucleotides(8). A large number of studies have revealed that lncRNAs are closely involved in the progression of human diseases, including growth, proliferation, invasion and migration(9–11). LncRNA TSIX has been identified to play crucial regulatory functions or serves as potential biomarkers in human cancers. For instance, TSIX promotes osteoblast apoptosis in particle-induced osteolysis via sponging and downregulating the expression of miR-30a-5(12). It was reported that TSIX was significantly upregulated in scleroderma dermal fibroblasts and regulated the stabilization of collagen mRNA(13).

Inhibition of TSIX can accelerate tibia fraction healing through binding and positively regulating the SOX6 expression(14). One previous study revealed that the panel of three RNAs including TSIX, miR-548-a-3p and SOGA1-based signatures show a higher specificity and sensitivity to separate HCC patients from control subjects, confirming its important diagnostic values(15). Despite these above, the roles of TSIX in NPC has not been reported and attracted to investigate its underlying mechanism *in vitro* and *in vivo*.

MicroRNAs (miRNAs) are a group of short non-coding RNAs approximately 20 nucleotides that always post-transcriptionally modulate gene expression through binding to the 3'-UTR of target mRNAs(16). MicroRNA-342-3p has been found to be frequently dysregulated in human cancers including NPC. The downregulation of miR-342-3p can exacerbate the aggressive phenotype in NPC cells by directly targeting Forkhead box 1 (FOXQ1)(17). In addition, miR-342-3p inhibits the progression of NPC cells by targeting and downregulating Cdc42 expression(18). However, the specific mechanism of miR-342-3p in NPC is lack and needed to be explored in detail.

Anterior Gradient 2 (AGR2) is a member of protein disulfide isomerase family and recent studies have revealed its varying oncogenic roles in cancer biology(19–21). In breast cancer (BC), high expression of AGR2 has an unfavorable impact on overall survival of patients with BC(22). Meanwhile, upregulation of AGR2 can attenuate the sensitivity of BC cells to fulvestrant and epirubicin(23, 24). In NPC, AGR2 has been found obviously increased in the serum of tumor patients, and suggested that AGR2 can potentially serves as a potential marker for the diagnose and prognosis of NPC(25). In addition, N, N' -dinitrosopiperazine-mediated AGR2 has been identified to be closely associated with the metastasis of NPC(26). These studies all confirmed the oncogenic roles of AGR2 in human cancers including NPC.

Here, we firstly found that TSIX was markedly upregulated in NPC tissues compared with matched normal tissues. Further, our results demonstrated that TSIX promoted the progression of NPC through upregulating AGR2 expression by sponging miR-342-3p, suggesting that TSIX might be a potential therapeutic target for NPC.

Methods

Tissues specimens

A total of 55 NPC tissues samples and 48 matched adjacent tissues samples were obtained by surgery from patients who suffered NPC and underwent the biopsy of the nasopharynx at The First Affiliated Hospital, Jinan University from March 2015 to March 2017. The diagnosis of NPC patients was pathologically confirmed according to the criteria of World Health Organization (WHO), and all chosen patients were informed with consent before surgery. The available samples were immediately snap frozen in liquid nitrogen and then stored at 80°C. This study was approved by the human Ethics Committee of National Engineering Research Center of Genetic Medicine.

Cell culture

Human NPC cell lines including SUNE1, HK1, CNE1 and CNE2 cells and normal nasopharyngeal epithelial cell NP69 cells were purchased from the Cell Bank of the Chinese Academy of Sciences. Cell were cultured with RPMI 1640 medium containing 10% FBS, 1% penicillin/streptomycin with 5% CO_2 at 37˚C.

Cell transfection

Cell transfection was performed in SUNE1 or HK1 cells by using Lipofectamine 3000 kit. Of which, sh-TSIX, sh-NC, miR-342-3p mimics, miR-NC, miR-inhibitor, inhibitor NC and sh-AGR2 were purchased from GenePharma Co., Ltd. Suzhou. In addition, to overexpress TSIX, the entire TSIX sequence was amplified and cloned into the pcDNA3.1 vector (GenePharma) to generate the overexpressing vector pc-TSIX, with empty vector pcDNA3.1 as the negative control. The sequences as follows: sh-TSIX: 5'-CAATCTCGCAAGATC CGGTG-3'; sh-AGR2: 5'-AGA GAT ACC ACAGTC AAA CC-3'; sh-NC (AGR2): 5'-AAC AGT CGC GTT TGC GAC TGG-3'.

miR-342-3p mimics and inhibitors were obtained from Gene-Pharma (Suzhou, China) (mimic: 5-UCUCACACAGAAAUCGCACCCGU-3’; inhibitor:5-ACGGGUGCGAUUUCUGUGUGAGA-30) The NC sequence is 5'-ACAAAGUUCUGUGAUGCACUGA-3' and 5'-ACAAAGUUCUGUGAUGCACUGA-3'

Luciferase reporter assay

The wile type (WT) or mutant type (MUT) fragments of TSIS or AGR2 containing the putative binding sites of miR-342-3p was obtained by PCR from human genome, and cloned into the pmirGLO Dual-Luciferase miRNA Target Expression Vector (Promega Corp., Fitchburg, WI, USA). Then SUNE1 cells were co-transfected with WT or MUT TSIX/AGR2 and miR-342-3p mimics or miR-NC by using the Lipofectamine 3000 kit. After transfection for 48 h, cells were collected, lysed and the relative luciferase activity was detected by using the Dual-Luciferase Assay system (Promega).

RNA isolation and qRT-PCR

Total RNA from tissues and cultured cells was extracted by TRIzol reagent (Invitrogen) according to the manufacturer's instructions. Reverse transcription was carried out by using the M-MLV reverse transcriptase kit (Promega, Madison, USA). The quantitative real-time PCR (qRT-PCR) was performed using the Bio-Rad CFX96 Touch sequence detection system (Bio-Rad Laboratories Inc., Hercules, CA, USA) based on the Platinum SYBR Green qPCR SuperMix-UDG reagents (Invitrogen), with GAPDH and U6 was considered as the internal reference. The relative fold changes of targets were analyzed by using $2^{-\Delta\Delta Ct}$ method(27). All primers using in this study as follows: AGR2 forward: 5'-TGATGGCCAGTATGTCCC-3', reverse: 5'-CAGTCTTCAGCAACTTGAG-3'; GAPDH forward: 5'-GAGTCAACG-GATTTGGTCGT -3', reverse: 5'-TTGATTTTGGAGGGATCTCG -3'; miR-342-3p forward: 5'-GGGTCTCACACAGAAATCGC-3', reverse: 5'-

CAGTGCGTGTCGTGGAGT-3'; U6 forward: 5'-CGCGCTTCGGCAGCACATATACT-3', reverse: 5'-ACGCTTCACGAATTTGCGTGTC-3'.

Western blot

Total protein of tissues or cultured cells was isolated by using RIPA lysis buffer (Beyotime Biotechnology, Shanghai, China) according to the manufacturer's instructions. Approximately equal amounts of protein were separated by 12% SDS-PAGE and then transferred nitrocellulose membrane based on the wet transfer method. After blocking with 3% skim milk, the membranes were incubated with primary antibodies against AGR2 (1:1000, ab209224, abcam) and internal reference GAPDH (1:2000, ab37168, abcam) 4°C overnight. On the following day, the membranes were incubated with goat anti-rabbit IgG (1:1000, ab6721, abcam) for 1 h which was diluted with 5% skim milk. After washing, the membranes were exposed to ECL solution followed by imaging by a Bio-Rad gel imaging system (MG8600; Thmorgan Biotechnology, Beijing, China). The gray values of target proteins were quantified by IPP7.0 software.

RIP assay

To determine the interaction between TSIX and miR-342-3p, RIP assay was performed by using the EZ-Magna RIP kit according to the manufacturer's instructions. In brief, cells were harvested, and the extraction was incubated with Ago2 antibody (5 μg/sample; Abcam, Cambridge, UK) with IgG was the negative control. Then co-precipitated RNAs were purified by using TRIzol reagent and the expression of TSIX or miR-342-3p was detected by qRT-PCR.

CCK-8 assay

Cell viability was evaluated by using Cell Counting Kit-8 (Dojindo, Kyushu, Japan). Briefly, approximately 1×10^3 cells were plated into 96-well plates for different times including 24h, 48h, 72h and 96h. Subsequently, 10 μl of CCK-8 solution was added into each well and incubated at 37°C for 2 h, then the absorbance was recorded at 450 nm to determine the cell viability.

Transwell assay

The Transwell assay was performed as previous described(28). Briefly, 3×10^4 cells with different treatments were added in the upper uncoated (migration) or 8.0-μm-pore Matrigel™-coated membranes (for invasion) with serum-free medium. Simultaneously, the lower chamber was filled with medium supplemented with 10% FBS. The chamber was cultured for 48 h to perform the migration assay and extracellular matrix gel was used for the cell invasion assay. Finally, cells were fixed by 4% paraformaldehyde and stained with crystal violet, then the cells were observed under the phase contrast microscope (×100 magnification) (Nikon) in 10 randomly fields.

Apoptosis analysis

Cell apoptosis was evaluated by using the Annexin V-FITC Apoptosis Detection Kit (Sangon Biotech). Briefly, cells with different treatments were re-suspended with 100 μL binding buffer. Then cells were double stained by Annexin V for 15 min and propidium iodide (PI) for 10 min. Afterwards, the apoptotic rate was evaluated by using BD LSRII Flow Cytometer System (BD Biosciences) and the data was quantitated with the FACSDiva Software.

EdU staining assay

To evaluate the proliferation of NPC cells with different treatments, Edu staining assay was performed using Cell-Light EdU Apollo 567 In Vitro Imaging Kit (Ribobio) as previously described(29). In brief, approximately 4×10^3 cells with different treatments in logarithmic phase were plated into 96-well plates. After 24 h, 100 μl medium containing 50 μM EdU was added into each well and incubated for 2 h at 37 °C. Then cells were fixed with 4% paraformaldehyde, and stained with Hoechst 33,342 and Apollp reaction cocktail. Images were captured by using a confocal LSM 710 (Carl Zeiss Microimaging, Jena, Germany) (×100 magnification) and EdU-positive cells were counted within each field by using ImageJ software.

Animal model

All male BALB/C nude mice (approximately 16-28g, 5-6 weeks) were purchased from The First Affiliated Hospital, Jinan University Laboratory Animal Technology Co., Ltd. and kept in a pathogen-free facility. Mice were anaesthetized with 0.1 ml/100 g pentobarbital sodium through intramuscular injection, and approximately 5×10^6 cells with different treatments were subcutaneously inoculated into the dorsal of the nude mice for *in vivo* xenograft assay. All mice were randomly divided into three groups: sh-NC group, sh-TSIX group, sh-TSIX + miR-342-3p inhibitor group. Tumor volume of different mice were calculated every 7 days for 28 days by the formula: volume = (length x width x width)/2. After kept 28 days, mice were sacrificed by cervical dislocation. Xenograft tumors from different groups were removed and weighted, meanwhile, the representative images of xenograft tumors were captured by a microscope. All animal producers were approved by the animal Ethics Committee of National Engineering Research Center of Genetic Medicine.

Immunohistochemistry

Paraffin-embedded tissues were deparaffinized, hydrated in ethyl alcohol and incubated with 0.3% H_2O_2 for elimination of endogenous peroxidase activity. After rupture of nuclear membrane with 0.1% Triton X-100 for 30 min and blockage with 5% normal donkey serum, tissue slides were incubated with primary antibody anti-Ki67 (abcam, Cambridge MA) at 4°C overnight and corresponding secondary antibody at

room temperature for 1 h. Immunohistochemistry results were captured using Olympus BX 41 Microscope (Olympus Corporation, Japan) (× 200 magnification).

Statistical analysis

All data were presented as mean ± SD which were derived from at least three independent experiments. Difference between two groups was determined by Student's t-test and difference among multiple groups was determined by one-way ANOVA. $P < 0.05$ was considered to be the significant threshold.

Results

LncRNA TSIX was significantly upregulated in NPC tissues and cell lines

To explore the roles of TSIX in NPC, the expression of TSIX in NPC tissues of patients with different clinicopathological features and corresponding cell lines was evaluated and the results showed that TSIX was significantly upregulated both in NPC tissues of patients with I + II stage ($p < 0.05$) and that with III + III stage ($p < 0.01$) compared with that in the adjacent tissues, and the increased expression of TSIX was positively associated with the pathological stage of NPC (Fig. 1A). To determine the effect of TSIX, we also evaluated its expression in NPC cell lines, and the results indicated that the expression of TSIX was also upregulated in several cell lines including SUNE1 ($p < 0.01$), HK1($p < 0.01$), CNE1 ($p < 0.05$) and CNE2 cells ($p < 0.05$) compared with normal nasopharyngeal epithelial cell NP69 cells (Fig. 1B). Meanwhile, it showed the highest expression of TSIX in SUNE1 and HK1 cells (Fig. 1B), so SUNE1 and HK1 cells were selected for the subsequent experiments. These results indicated that TSIX might be positively related to the progression of NPC.

Downregulation of TSIX efficiently inhibited NPC progression

To explore the function of TSIX in NPC, pc-TSIX (overexpression of TSIX) or negative control pcDNA3.1 and sh-TSIX (silencing of TSIX) or negative control sh-NC was transfected into SUN1 and HK1 cells. qRT-PCR assay showed that pc-TSIX significantly increased the expression of TSIX both in SUN1 and HK1 cells compared with pcDNA3.1 control ($p < 0.05$), while sh-TSIX markedly decreased the expression of TSIX both in SUN1 and HK1 cells compared with sh-NC control ($p < 0.05$) (Fig. 2A), suggesting that pc-TSIX and sh-TSIX could be used for the subsequent experiments. The results of CCK-8 assay indicated that overexpression of TSIX significantly promoted the cell viability of SUN1 and HK1 cells compared with pcDNA3.1 control ($p < 0.01$), while downregulation of TSIX significantly inhibit the cell viability of SUN1 and HK1 cells compared with sh-NC group ($p < 0.05$) (Fig. 2B). For cell apoptosis, silencing of TSIX significantly promoted the apoptosis of both SUN1 and HK1 cells ($p < 0.01$), while no obvious effect in

the pc-TSIX group both in SUN1 and HK1 cells (Fig. 2C). Meanwhile, EdU staining assay showed that overexpression of TSIX significantly increased the EdU positive cells of both SUN1 and HK1 cells compared with pcDNA3.1 control group ($p < 0.05$), while silencing of TSIX markedly decreased the numbers of EdU positive cells of both SUN1 and HK1 cells compare with sh-NC group ($p < 0.05$) (Fig. 2D). In addition, our results also showed that overexpression of TSIX significantly promoted the invasion ($p < 0.05$) and migration ($p < 0.05$) of SUN1 and HK1 cells compared with pcDNA3.1 control group, while silencing of TSIX obviously inhibited the invasion ($p < 0.05$) and migration ($p < 0.05$) of SUN1 and HK1 cells compared with sh-NC group (Fig. 2E). These results indicated that downregulation of TSIX could inhibit the development of NPC which was characterized by decreased cell viability, proliferation, invasion and migration of NPC cells, while upregulation of TSIX oppositely exacerbated NPC progression.

TSIX acted as a ceRNA of miR-342-3p

To explore the specific mechanism of TSIX in NPC, StarBase v2.0 was used to predicted the potential targets of TSIX, and the results showed that there was a putative binding site between TSIX and miR-342-3p (Fig. 3E), suggesting that TSIX might act as a ceRNA of miR-342-3p. To determine the interaction between TSIX and miR-342-3p, SUN1 cells was transfected with pc-TSIX, pcDNA3.1, sh-TSIX or sh-NC, and qRT-PCR assay showed that overexpression of TSIX significantly decreased the expression of miR-342-3p compared with pcDNA3.1 group ($p < 0.05$), while silencing of TSIX dramatically increased miR-342-3p expression compared with sh-NC group ($p < 0.05$) (Fig. 3A). Moreover, we found that miR-342-3p was significantly downregulated in NPC tissues of patients with I + II stage ($p < 0.05$) and that with III + III stage ($p < 0.01$) compared with that in the adjacent tissues (Fig. 3B). Meanwhile, miR-342-3p was also downregulated in SUNE1 ($p < 0.01$), HK1($p < 0.01$), CNE1 ($p < 0.05$) and CNE2 cells ($p < 0.05$) compared with NP69 cells (Fig. 3C). Besides, Pearson correlation analysis showed that there was an obvious negative correlation between TSIX and miR-342-3p in NPC tissues ($R^2 = 0.56$, $p <. 001$) (Fig. 3D). To further confirm their relationship, the WT or MUT type TSIX against miR-342-3p (Fig. 3E) was co-transfected with miR-342-3p mimics or miR-NC into SUN1 cells and the luciferase reporter assay was performed. The results showed that miR-342-3p mimics significantly decreased the relative luciferase activity of WT TSIX ($p < 0.05$), while exhibited no obvious change in MUT TSIX (Fig. 3F). In addition, the results of RIP assay revealed that the relative expression level of TSIX or miR-342-3p was all significantly increased in anti-Ago2 group compared with IgG group ($p < 0.001$) (Fig. 3G). These data suggested that TSIX play its crucial roles in NPC through sponging miR-342-3p.

MiR-342-3p inhibitor reversed sh-TSIX induced inhibitory effect in NPC progression

To determine whether the inhibitory effect of sh-TSIX was mediated by miR-342-3p, SUN1 cells were transfected with sh-TSIX, sh-NC, or co-transfected with sh-TSIX and miR-342-3p inhibitor. We firstly evaluated the transfection efficiency of miR-342-3p inhibitor and the results showed that miR-342-3p

inhibitor significantly decreased the expression of miR-342-3p ($p < 0.01$). Further, miR-342-3p inhibitor significantly reversed sh-TSIX induced inhibitory effect in cell viability of SUN1 cells compared with sh-TSIX group ($p < 0.01$) (Fig. 4B). Additional miR-342-3p inhibitor obviously inhibited sh-TSIX induced apoptosis of SUN1 cells compared with sh-TSIX group ($p < 0.05$) (Fig. 4C). Meanwhile, co-transfection sh-TSIX and miR-342-3p inhibitor also significantly reversed sh-TSIX induced inhibitory effect on the numbers of EdU positive cells in SUN1 cells compared with sh-TSIX group ($p < 0.05$) (Fig. 4D). In addition, the results of transwell assay showed that miR-342-3p inhibitor significantly reversed sh-TSIX induced inhibitory effect on the invasion ($p < 0.05$) and migration ($p < 0.05$) of SUN1 cells compared with sh-TSIX group (Fig. 4E). These results revealed that downregulation of miR-342-3p could efficiently reversed sh-TSIX induced inhibitory effect in NPC progression.

AGR2 was a target of miR-342-3p

Next, Targetscan ATG14 (http://www.targetscan.org/cgi-bin/targetscan/vert_71/) was applied to predicted the potential targets of miR-342-3p, and the results showed that AGR2 might be a potential target of miR-342-3p (Fig. 5A). To determine this prediction, the WT or MUT AGR2 fragments containing putative binding site of miR-342-3p was cloned into luciferase reporter vector and the luciferase assay indicated that overexpression of miR-342-3p significantly decreased the relative luciferase activity of WT type AGR2 ($p < 0.05$), while showed no obvious change in MUT AGR2 (Fig. 5B). Further, SUN1 cells were transfected with miR-342-3p mimics, miR-NC, miR-342-3p inhibitor, or inhibitor NC, and the expression of AGR2 was evaluated by western blot. The results showed that miR-342-3p mimics significantly decreased the protein expression of AGR2 compared with miR-NC group ($p < 0.05$), while miR-342-3p inhibitor obviously increased AGR2 expression ($p < 0.05$) (Fig. 5C). Meanwhile, SUN1 cells were then transfected with pc-TSIX, pcDNA3.1, sh-TSIX or sh-NC, and the protein expression of AGR2 was also evaluated by western blot. The results indicated that overexpression of TSIX significantly increased the protein level of AGR2 compared with pcDNA3.1 control ($p < 0.05$), while silencing of TSIX decreased the AGR2 expression ($p < 0.05$) (Fig. 5D). In addition, we also explore whether downregulation of AGR2 could reversed the effect of miR-342-3p inhibitor in NPC progression. Hence, SUN1 cells were transfected with sh-AGR2 or sh-NC (AGR2), and qRT-PCR assay revealed that sh-AGR2 could significantly decreased the mRNA expression of AGR2 compared with sh-NC group ($p < 0.01$). Moreover, downregulation of AGR2 could markedly inhibited the cell viability ($p < 0.05$) (Fig. 5F) and proliferation ($p < 0.05$) (Fig. 5G) of SUN1 cells induced by miR-342-3p inhibitor compared with sh-NC group. These results demonstrated that the effect of miR-342-3p in NPC was mediated by AGR2.

Downregulation of TSIX inhibited tumor development *in vivo* through targeting miR-342-3p/AGR2 axis

Finally, the tumor xenograft mice model of NPC *in vivo* was established to confirm the role of TSIX. The results indicated that sh-TSIX efficiently decreased the tumor volume of xenograft tumor in mice

compared with sh-NC group ($p < 0.05$), while miR-342-3p inhibitor obviously reversed the inhibitory effect of sh-TSIX ($p < 0.01$) (Fig. 6A). Meanwhile, sh-TSIX efficiently decreased the tumor weight of xenograft tumor in mice ($p < 0.01$), while downregulation of miR-342-3p could obviously reversed sh-TSIX induced protective effect ($p < 0.05$) (Fig. 6B). The representative images of xenograft tumor from different groups were shown in Fig. 6C. As expected, the results of Ki-67 staining assay in tumor tissues showed that sh-TSIX could significantly reduce the proliferation of NPC cells compared with sh-NC group, while miR-342-3p inhibitor obviously reversed the inhibitory effect of sh-TSIX (Fig. 6D). Moreover, the protein expression of AGR2 in tumor tissues was evaluated, and the results indicated that sh-TSIX significantly decreased the protein expression of AGR2 compared with sh-NC group ($p < 0.05$), while co-transfection of sh-TSIX and miR-342-3p inhibitor obviously reversed the inhibitory effect of sh-TSIX on AGR2 expression ($p < 0.05$) (Fig. 6E). These results indicated that downregulation of TSIX could efficiently inhibit tumor development *in vivo* through targeting miR-342-3p/AGR2 axis.

Discussion

Increasing evidences indicated that most NPC-caused death are due to its recurrence or metastasis(30). Therefore, it is essential to understand the specific mechanisms during NPC development. Recently, a series of lncRNAs have been identified to exert vital biological functions in NPC, which might be considered as potential biomarkers. LncRNA NKILA suppresses the carcinogenesis and metastasis of NPC through inactivating the NF-κB signaling pathway(31). LncRNA THOR has been found that can attenuate cisplatin sensitivity of NPC cells via enhancing cells stemness(32). LncRNA HOTAIR contributes to the tumorigenesis of NPC via targeting and upregulating FASN expression(33). LncRNA DANCR can stabilizes HIF-1α and exacerbate the metastasis in NPC through directly targeting NF90/NF45 axis(34). Liu et al. have demonstrated that increased expression of lncRNA SNHG12 potentially predicts a poor prognosis of NPC and promotes the development of NPC via modulating Notch signal pathway(35). LncRNA ROR can promote proliferation, migration and chemoresistance of NPC cells, and suggested it might be regarded as a therapeutic target and potentially reduce chemoresistance of NPC(36). Although lncRNA TSIX has been revealed to act as crucial roles in various cancers, its function in NPC remains unclear. Here, we found that TSIX was markedly upregulated in NPC tissues with different clinicopathological features and several NPC cell lines. Moreover, silencing of TSIX could efficiently inhibit the viability, growth, invasion, migration, and induce apoptosis of NPC cells, while overexpression of TSIX significantly exacerbated NPC progression. These data suggested that TSIX might play a potential oncogenic role in NPC.

It has been reported that lncRNAs always play their important roles by directly sponging miRNAs in the development and progression of human cancers including NCP(37, 38). In NPC, several lncRNAs have been identified to directly sponge miRNAs to promote or inhibit the progression of NPC. For example, LINC00210 can sponge miR-328-5p to promote NPC tumorigenesis through activating NOTCH3 signaling pathway(39). Knockdown of lncRNA ZFAS1 can efficiently suppress the progression of NPC through sponging miR-135a(40). Silencing of lncRNA ANRIL significantly inhibit the proliferation, induces apoptosis, and promotes the radiosensitivity in NPC cells by directly targeting miR-125a and then

upregulating its expression(41). In addition, upregulation of lncRNA HAGLROS can efficiently promote the development of NPC by modulating PI3K/AKT/mTOR signaling pathways through targeting miR-100/ATG14 axis(42). Here, to explore the specific mechanisms of TSIX in NPC, Starbase v2.0 database was used to predicted the potential targets of TSIX, and showed that there was a putative binding site between TSIX and miR-342-3p, suggesting that miR-342-2p might be a target of TSIX. Further, luciferase reporter assay and RIP assay all confirmed the negative correlation between TSIX and miR-342-3p. Meanwhile, downregulation of miR-342-3p could significantly reverse sh-TSIX induced inhibitory effect in NPC development including cell viability, proliferation, invasion, migration and apoptosis.

MiRNAs have also been identified to play crucial roles in the progression of cancer through directly binding to the 3'UTR of targets mRNA(43, 44). To perfect the regulatory network of TSIX/miR-342-3p axis in NPC, Targetscan was applied to search for the potential targets of miR-342-3p, and the results suggested that miR-342-3p might directly bind to the 3'UTR of AGR2. Meanwhile, the luciferase assay showed that overexpression of miR-342-3p could obviously decrease the relative luciferase activity of WT type AGR2, while showed no obvious change in MUT AGR2. In addition, miR-342-3p mimics significantly decreased the expression of AGR2, while miR-342-3p inhibitor obviously increased AGR2 expression in SUN1 cells; Overexpression of TSIX significantly increased the expression of AGR2, while silencing of TSIX decreased the AGR2 expression. These data suggested that miR-342-3p could negatively regulate AGR2 by directly binding to the 3'UTR of AGR2. Based on previous studies of AGR2 in NPC that, the expression of AGR2 was significantly overexpressed and high AGR2 expression was associated with NPC metastasis(26). The *in vivo* experiments in xenograft mice model was performed and the results indicated that sh-TSIX significantly decreased the protein expression of AGR2 compared with sh-NC group in tumor tissues, while co-transfection of sh-TSIX and miR-342-3p inhibitor obviously reversed the inhibitory effect of sh-TSIX on AGR2 expression. Moreover, downregulation of TSIX efficiently inhibit the tumor development in mice, and this inhibitory effect was obviously reversed by miR-342-3p inhibitor. All these results suggested that downregulation of TSIX could efficiently attenuate NPC progression through targeting miR-342-3p/AGR2 axis.

However, whether the effect of TSIX or miR-342-3p in NPC could be affected by AGR2 should be confirmed in the subsequent experiments in the future.

Conclusion

In this study, we discovered a novel mechanism of lncRNA TSIX in NPC progression, that was, TSIX promoted the development of NPC through upregulating AGR2 expression by directly sponging miR-342-3p, providing a potential therapeutic target for NPC.

Declarations

Ethical Approval and Consent to participate

All chosen patients were informed with consent before surgery. All producers were approved by the human Ethics Committee of National Engineering Research Center of Genetic Medicine. Procedures operated in this research were completed in keeping with the standards set out in the Announcement of Helsinki and laboratory guidelines of research in China. All animal producers were approved by the animal Ethics Committee of National Engineering Research Center of Genetic Medicine.

Consent to publish

Not applicable.

Availability of data and material

The data that support the findings of this study are available on request from the corresponding author.

The data are not publicly available due to their containing information that could compromise the privacy of research participants.

Competing interests

All other authors have no conflicts of interest.

We declare that we do not have any commercial or associative interest that represents a conflict of interest in connection with the work submitted.

Funding

Not Applicable.

Authors' contributions

SPC, XXH: study concepts, literature research, clinical studies, data analysis, experimental studies, manuscript writing and review; QXZ, ZS: study design, literature research, experimental studies and manuscript editing; ZYL, XTQ, ZW: definition of intellectual content, clinical studies, data acquisition and statistical analysis; HML, KLM, SYW: data acquisition, manuscript preparation and data analysis; YYL, DW: data acquisition and statistical analysis.

All authors have read and approve the submission of the manuscript.

Acknowledgements

Not Applicable.

References

1. Petersson F. Nasopharyngeal carcinoma: a review. Seminars in diagnostic pathology. 2015;32(1):54-73.
2. Kamran SC, Riaz N, Lee N. Nasopharyngeal carcinoma. Surgical oncology clinics of North America. 2015;24(3):547-61.
3. Chen YP, Chan ATC, Le QT, Blanchard P, Sun Y, Ma J. Nasopharyngeal carcinoma. Lancet (London, England). 2019;394(10192):64-80.
4. Lee AW, Ma BB, Ng WT, Chan AT. Management of Nasopharyngeal Carcinoma: Current Practice and Future Perspective. Journal of clinical oncology : official journal of the American Society of Clinical Oncology. 2015;33(29):3356-64.
5. Chou J, Lin YC, Kim J, You L, Xu Z, He B, et al. Nasopharyngeal carcinoma--review of the molecular mechanisms of tumorigenesis. Head & neck. 2008;30(7):946-63.
6. Chen ZT, Liang ZG, Zhu XD. A Review: Proteomics in Nasopharyngeal Carcinoma. International journal of molecular sciences. 2015;16(7):15497-530.
7. Razak AR, Siu LL, Liu FF, Ito E, O'Sullivan B, Chan K. Nasopharyngeal carcinoma: the next challenges. European journal of cancer (Oxford, England : 1990). 2010;46(11):1967-78.
8. Morris KV, Mattick JS. The rise of regulatory RNA. Nature reviews Genetics. 2014;15(6):423-37.
9. Yarmishyn AA, Kurochkin IV. Long noncoding RNAs: a potential novel class of cancer biomarkers. Frontiers in genetics. 2015;6:145.
10. Ulitsky I, Bartel DP. lincRNAs: genomics, evolution, and mechanisms. Cell. 2013;154(1):26-46.
11. Saxena A, Carninci P. Long non-coding RNA modifies chromatin: epigenetic silencing by long non-coding RNAs. BioEssays : news and reviews in molecular, cellular and developmental biology. 2011;33(11):830-9.
12. Bu Y, Zheng D, Wang L, Liu J. LncRNA TSIX promotes osteoblast apoptosis in particle-induced osteolysis by down-regulating miR-30a-5p. Connective tissue research. 2018;59(6):534-41.
13. Wang Z, Jinnin M, Nakamura K, Harada M, Kudo H, Nakayama W, et al. Long non-coding RNA TSIX is upregulated in scleroderma dermal fibroblasts and controls collagen mRNA stabilization. Experimental dermatology. 2016;25(2):131-6.
14. Xu WW, Xu Y, Ji F, Ji Y, Wang QG. Inhibition of long non-coding RNA TSIX accelerates tibia fraction healing via binding and positively regulating the SOX6 expression. European review for medical and pharmacological sciences. 2020;24(8):4070-9.
15. Habieb A, Matboli M. Potential role of lncRNA-TSIX, miR-548-a-3p, and SOGA1 mRNA in the diagnosis of hepatocellular carcinoma. 2019;46(4):4581-90.
16. Wang J, Ye H, Zhang D, Cheng K, Hu Y, Yu X, et al. Cancer-derived Circulating MicroRNAs Promote Tumor Angiogenesis by Entering Dendritic Cells to Degrade Highly Complementary MicroRNAs.

Theranostics. 2017;7(6):1407-21.

17. Cui Z, Zhao Y. microRNA-342-3p targets FOXQ1 to suppress the aggressive phenotype of nasopharyngeal carcinoma cells. BMC cancer. 2019;19(1):104.
18. Shi L, Xiao R, Wang M, Zhang M, Weng N, Zhao X, et al. MicroRNA-342-3p suppresses proliferation and invasion of nasopharyngeal carcinoma cells by directly targeting Cdc42. Oncology reports. 2018;40(5):2750-7.
19. Xiu B, Chi Y, Liu L, Chi W, Zhang Q, Chen J, et al. LINC02273 drives breast cancer metastasis by epigenetically increasing AGR2 transcription. 2019;18(1):187.
20. Dumartin L, Alrawashdeh W, Trabulo SM, Radon TP, Steiger K, Feakins RM, et al. ER stress protein AGR2 precedes and is involved in the regulation of pancreatic cancer initiation. Oncogene. 2017;36(22):3094-103.
21. Chevet E, Fessart D, Delom F, Mulot A, Vojtesek B, Hrstka R, et al. Emerging roles for the pro-oncogenic anterior gradient-2 in cancer development. Oncogene. 2013;32(20):2499-509.
22. Tian SB, Tao KX, Hu J, Liu ZB, Ding XL, Chu YN, et al. The prognostic value of AGR2 expression in solid tumours: a systematic review and meta-analysis. Scientific reports. 2017;7(1):15500.
23. Li Z, Zhu Q, Chen H, Hu L, Negi H, Zheng Y, et al. Binding of anterior gradient 2 and estrogen receptor-α: Dual critical roles in enhancing fulvestrant resistance and IGF-1-induced tumorigenesis of breast cancer. Cancer letters. 2016;377(1):32-43.
24. Li Z, Zhu Q, Hu L, Chen H, Wu Z. Anterior gradient 2 is a binding stabilizer of hypoxia inducible factor-1α that enhances CoCl2 -induced doxorubicin resistance in breast cancer cells. 2015;106(8):1041-9.
25. Li Y, Wang W, Liu Z, Jiang Y, Lu J, Xie H, et al. AGR2 diagnostic value in nasopharyngeal carcinoma prognosis. Clinica chimica acta; international journal of clinical chemistry. 2018;484:323-7.
26. Li Y, Lu J, Peng Z, Tan G, Liu N, Huang D, et al. N,N'-dinitrosopiperazine-mediated AGR2 is involved in metastasis of nasopharyngeal carcinoma. PloS one. 2014;9(4):e92081.
27. Livak KJ, Schmittgen TD. Analysis of relative gene expression data using real-time quantitative PCR and the 2(-Delta Delta C(T)) Method. Methods (San Diego, Calif). 2001;25(4):402-8.
28. Zheng YQ, Bai YF, Yang S, Cui YR, Wang YP, Hu WL. MircoRNA-629 promotes proliferation, invasion and migration of nasopharyngeal carcinoma through targeting PDCD4. European review for medical and pharmacological sciences. 2019;23(1):207-16.
29. Wu RS, Qiu EH, Zhu JJ, Wang JR, Lin HL. MiR-101 promotes nasopharyngeal carcinoma cell apoptosis through inhibiting Ras/Raf/MEK/ERK signaling pathway. European review for medical and pharmacological sciences. 2018;22(1):150-7.
30. Lee V, Kwong D, Leung TW, Lam KO, Tong CC, Lee A. Palliative systemic therapy for recurrent or metastatic nasopharyngeal carcinoma - How far have we achieved? Critical reviews in oncology/hematology. 2017;114:13-23.
31. Zhang W, Guo Q, Liu G, Zheng F, Chen J, Huang D, et al. NKILA represses nasopharyngeal carcinoma carcinogenesis and metastasis by NF-κB pathway inhibition. 2019;15(8):e1008325.

32. Gao L, Cheng XL, Cao H. LncRNA THOR attenuates cisplatin sensitivity of nasopharyngeal carcinoma cells via enhancing cells stemness. Biochimie. 2018;152:63-72.
33. Ma DD, Yuan LL, Lin LQ. LncRNA HOTAIR contributes to the tumorigenesis of nasopharyngeal carcinoma via up-regulating FASN. European review for medical and pharmacological sciences. 2017;21(22):5143-52.
34. Wen X, Liu X, Mao YP, Yang XJ, Wang YQ, Zhang PP, et al. Long non-coding RNA DANCR stabilizes HIF-1α and promotes metastasis by interacting with NF90/NF45 complex in nasopharyngeal carcinoma. Theranostics. 2018;8(20):5676-89.
35. Liu ZB, Tang C, Jin X, Liu SH, Pi W. Increased expression of lncRNA SNHG12 predicts a poor prognosis of nasopharyngeal carcinoma and regulates cell proliferation and metastasis by modulating Notch signal pathway. Cancer biomarkers : section A of Disease markers. 2018;23(4):603-13.
36. Li L, Gu M, You B, Shi S, Shan Y, Bao L, et al. Long non-coding RNA ROR promotes proliferation, migration and chemoresistance of nasopharyngeal carcinoma. Cancer science. 2016;107(9):1215-22.
37. Wu XS, Wang F, Li HF, Hu YP, Jiang L, Zhang F, et al. LncRNA-PAGBC acts as a microRNA sponge and promotes gallbladder tumorigenesis. 2017;18(10):1837-53.
38. Lei H, Gao Y, Xu X. LncRNA TUG1 influences papillary thyroid cancer cell proliferation, migration and EMT formation through targeting miR-145. Acta biochimica et biophysica Sinica. 2017;49(7):588-97.
39. Zhang S, Li P, Zhao L, Xu L. LINC00210 as a miR-328-5p sponge promotes nasopharyngeal carcinoma tumorigenesis by activating NOTCH3 pathway. Bioscience reports. 2018;38(6).
40. Wang M, Ji YQ, Song ZB, Ma XX, Zou YY, Li XS. Knockdown of lncRNA ZFAS1 inhibits progression of nasopharyngeal carcinoma by sponging miR-135a. Neoplasma. 2019;66(6):939-45.
41. Hu X, Jiang H, Jiang X. Downregulation of lncRNA ANRIL inhibits proliferation, induces apoptosis, and enhances radiosensitivity in nasopharyngeal carcinoma cells through regulating miR-125a. Cancer biology & therapy. 2017;18(5):331-8.
42. Zhang W, Zhang Y, Xi S. Upregulation of lncRNA HAGLROS enhances the development of nasopharyngeal carcinoma via modulating miR-100/ATG14 axis-mediated PI3K/AKT/mTOR signals. Artificial cells, nanomedicine, and biotechnology. 2019;47(1):3043-52.
43. Vishnoi A, Rani S. MiRNA Biogenesis and Regulation of Diseases: An Overview. Methods in molecular biology (Clifton, NJ). 2017;1509:1-10.
44. Wei YT, Guo DW, Hou XZ, Jiang DQ. miRNA-223 suppresses FOXO1 and functions as a potential tumor marker in breast cancer. Cellular and molecular biology (Noisy-le-Grand, France). 2017;63(5):113-8.

Figures

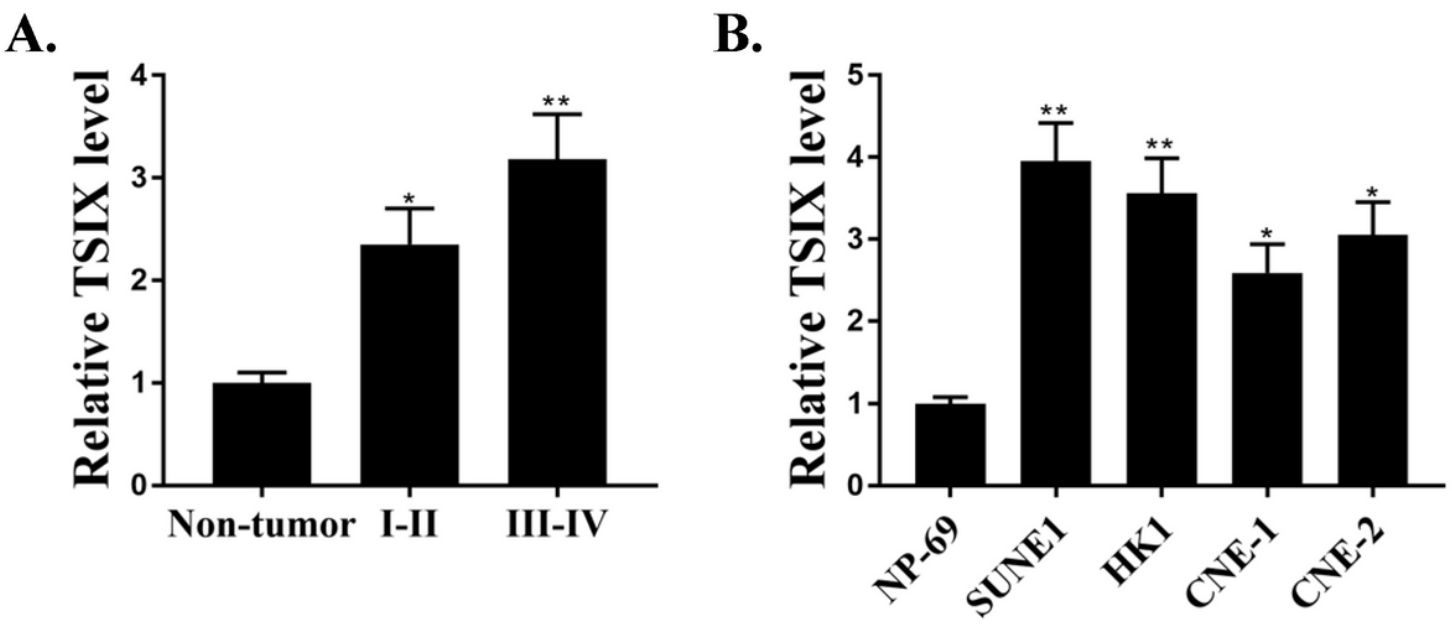

Figure 1

TSIX was significantly upregulated in NPC tissues and cell lines. (A) The mRNA level of TSIX in NPC tissues of patients different clinicopathological features and matched adjacent tissues was evaluated by qRT-PCR (adjacent tissues n = 48, stage I + II n = 26, stage III + III n = 29). (B) The mRNA expression of TSIX in NPC cell lines and normal nasopharyngeal epithelial cell NP69 was evaluated by qRT-PCR (n = 4). * $p < 0.05$, ** $p < 0.01$.

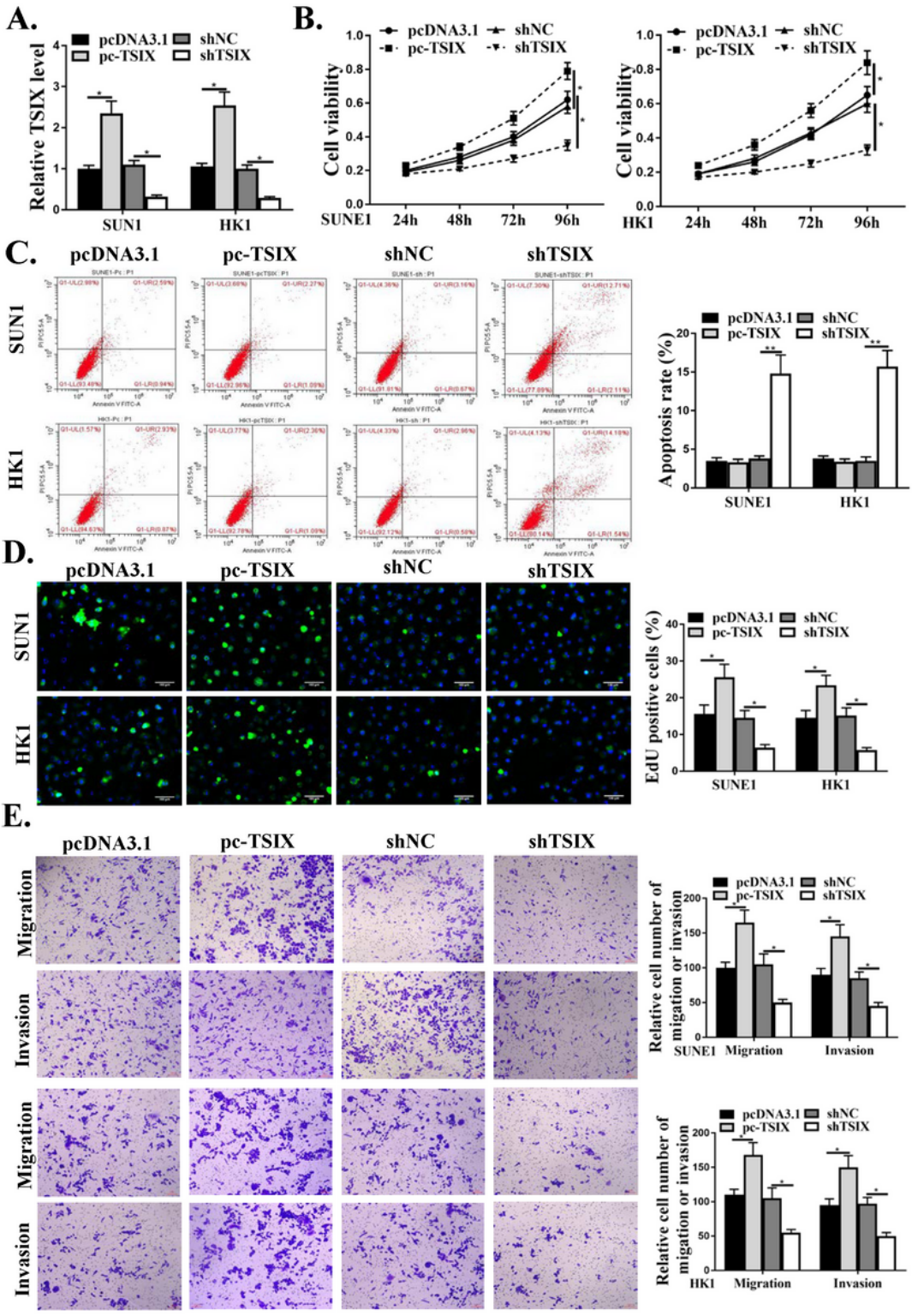

Figure 2

Downregulation of TSIX efficiently inhibited NPC progression. SUN1 and HK1 cells were transfected with pc-TSIX, pcDNA3.1, sh-TSIX or sh-NC. (A) The mRNA level of TSIX was evaluated by qRT-PCR. (B) Cell viability was detected by CCK-8 assay. (C) Cell apoptosis rate was evaluated by flow cytometry. (D) Cell proliferation was evaluated by EdU staining assay. Images were merged with green channel and blue channel. And the multiple supporting fields of cells were shown in Supplementary Figure 1. × 100

magnification, scale bar = 100 μm. (E) The cell numbers of invasion and migration was evaluated by Transwell assay. × 100 magnification, scale bar = 20 μm. N = 4, * p < 0.05, ** p < 0.01.

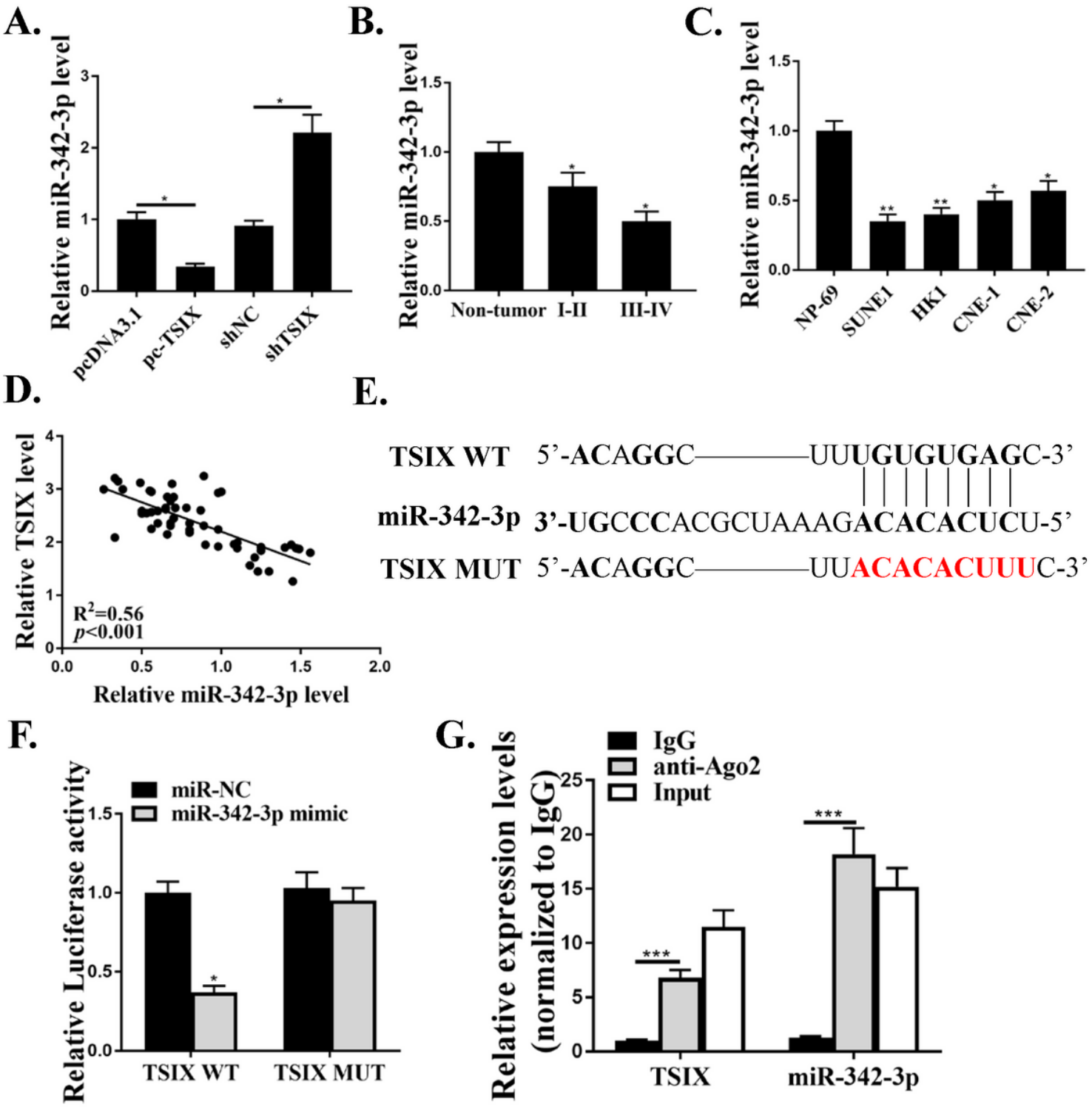

Figure 3

TSIX acted as a ceRNA of miR-342-3p. (A) SUN1 cells were transfected with pc-TSIX, pcDNA3.1, sh-TSIX or sh-N, and the mRNA expression of miR-342-3p was evaluated by qRT-PCR (n = 4). (B) The mRNA level of miR-342-3p in NPC tissues of patients different clinicopathological features and matched adjacent tissues was evaluated by qRT-PCR (adjacent tissues n = 48, stage I + II, n = 26, stage III + III, n = 29). (C)

The mRNA level of miR-342-3p in NPC cell lines and normal NP69 cells was evaluated by qRT-PCR (n = 4). (D) Pearson correlation analysis between the expression of TSIX and miR-342-3p (n = 55). (E) The potential targets of TSIX was predicted by StarBase v2.0. (F) The relative activity of WT or MUT TSIX was evaluated by luciferase reporter assay (n = 4). (G) The enrichment fold of TSIX or miR-342-3p was evaluated by RIP assay (n = 4). * p < 0.05, ** p < 0.01.

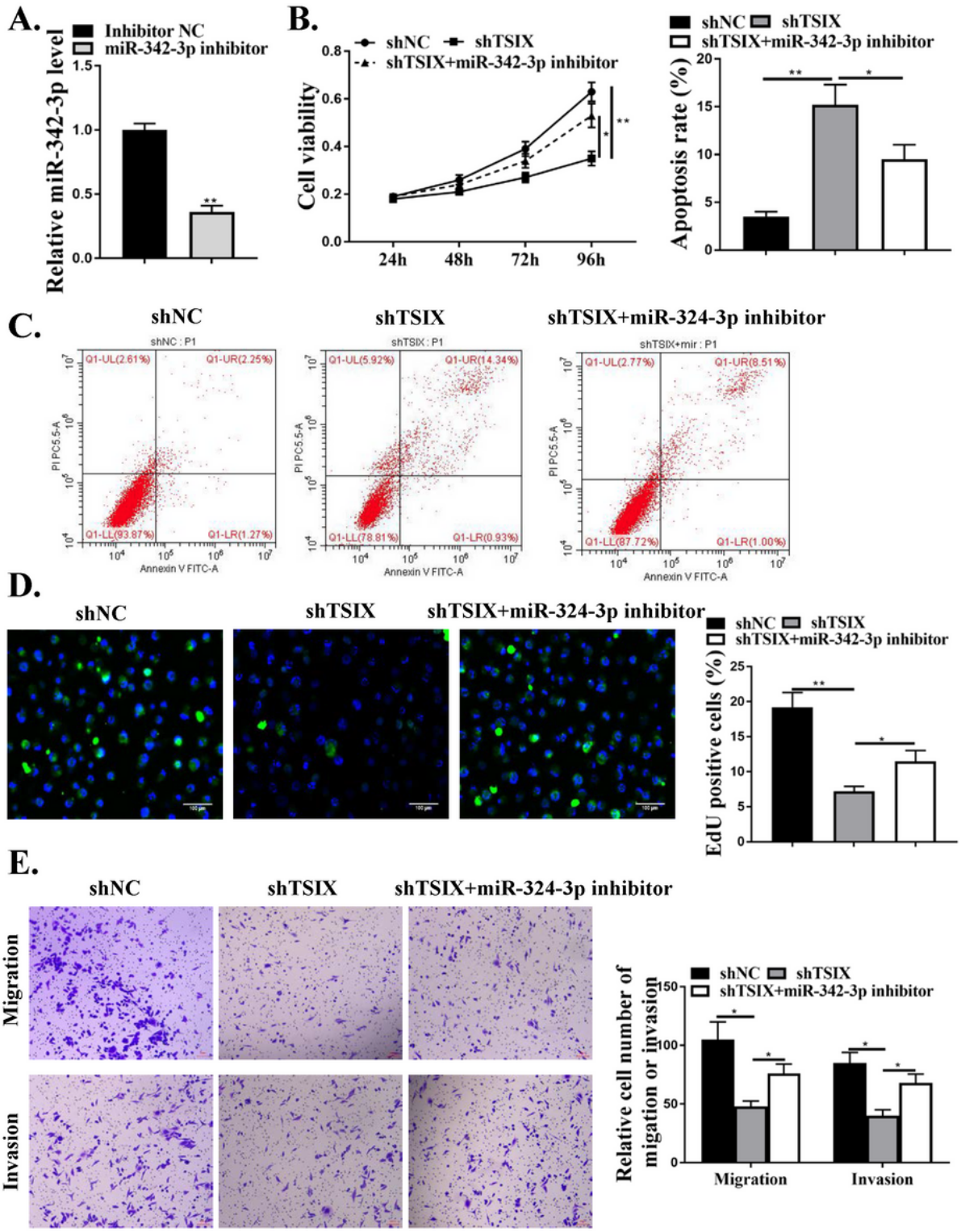

Figure 4

MiR-342-3p inhibitor reversed sh-TSIX induced inhibitory effect in NPC progression. (A) SUN1 cells were transfected with miR-342-3p inhibitor or inhibitor NC, and the mRNA level of miR-342-3p was evaluated by qRT-PCR. (B-E) SUN1 cells were transfected with sh-TSIX, sh-NC, or co-transfected with sh-TSIX and miR-342-3p inhibitor. (B) Cell viability was evaluated by CCK-8 assay. (C) Cell apoptosis rate was evaluated by flow cytometry. (D) Cell proliferation was evaluated by EdU staining assay. Images were merged with green channel and blue channel. And the multiple supporting fields of cells were shown in Supplementary Figure 2. × 100 magnification, scale bar = 100 μm. (E) The cell numbers of invasion and migration was evaluated by Transwell assay. × 100 magnification, scale bar = 20 μm. N = 4, * $p < 0.05$, ** $p < 0.01$.

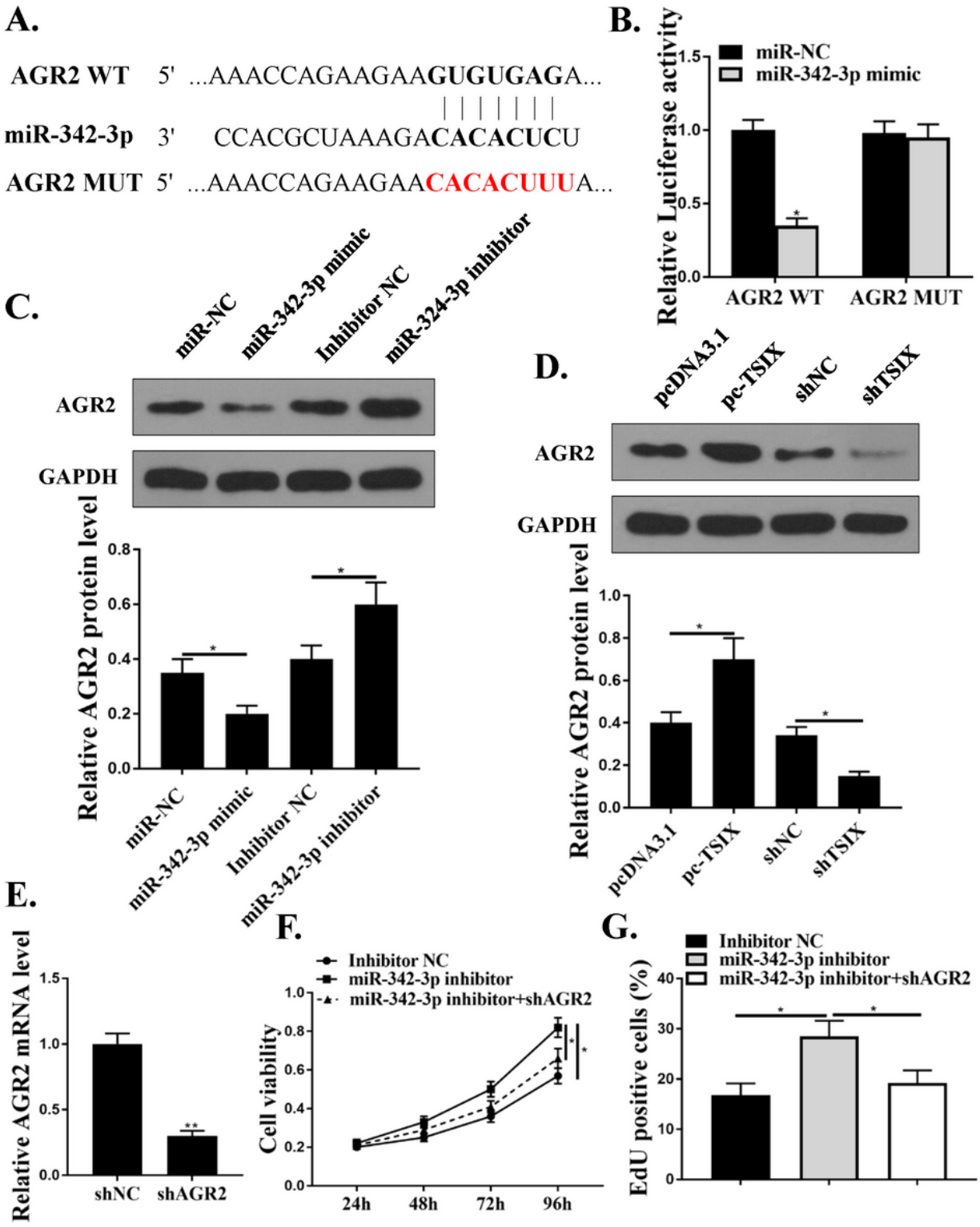

Figure 5

AGR2 was a target of miR-342-3p. (A) The putative binding site between miR-342-3p and AGR2 was predicted by Targetscan. (B) The WT or MUT type AGR2 was co-transfected with miR-342-3p mimics or miR-NC into SUN1 cells, and the relative luciferase activity was evaluated by dual luciferase reporter system (n = 4). (C) SUN1 cells were transfected with miR-342-3p mimics, miR-NC, miR-342-3p inhibitor, or inhibitor NC, and the protein level of AGR2 was evaluated by western blot. Full-length blots/gels are

presented in Supplementary Figure 3. (D) SUN1 cells were also transfected with pc-TSIX, pcDNA3.1, sh-TSIX or sh-NC, and the protein expression of AGR2 was evaluated by western blot. Full-length blots/gels are presented in Supplementary Figure 4. (E) SUN1 cells were transfected with sh-AGR2 or sh-NC, and the mRNA expression of AGR2 was evaluated by qRT-PCR. (F and G) SUN1 cells were transfected with miR-342-3p inhibitor, inhibitor NC, or co-transfected with miR-342-3p inhibitor and sh-AGR2. (F) Cell viability was evaluated by CCK-8 assay. (G) Cell proliferation was evaluated by EdU staining assay. N= 4, * p < 0.05.

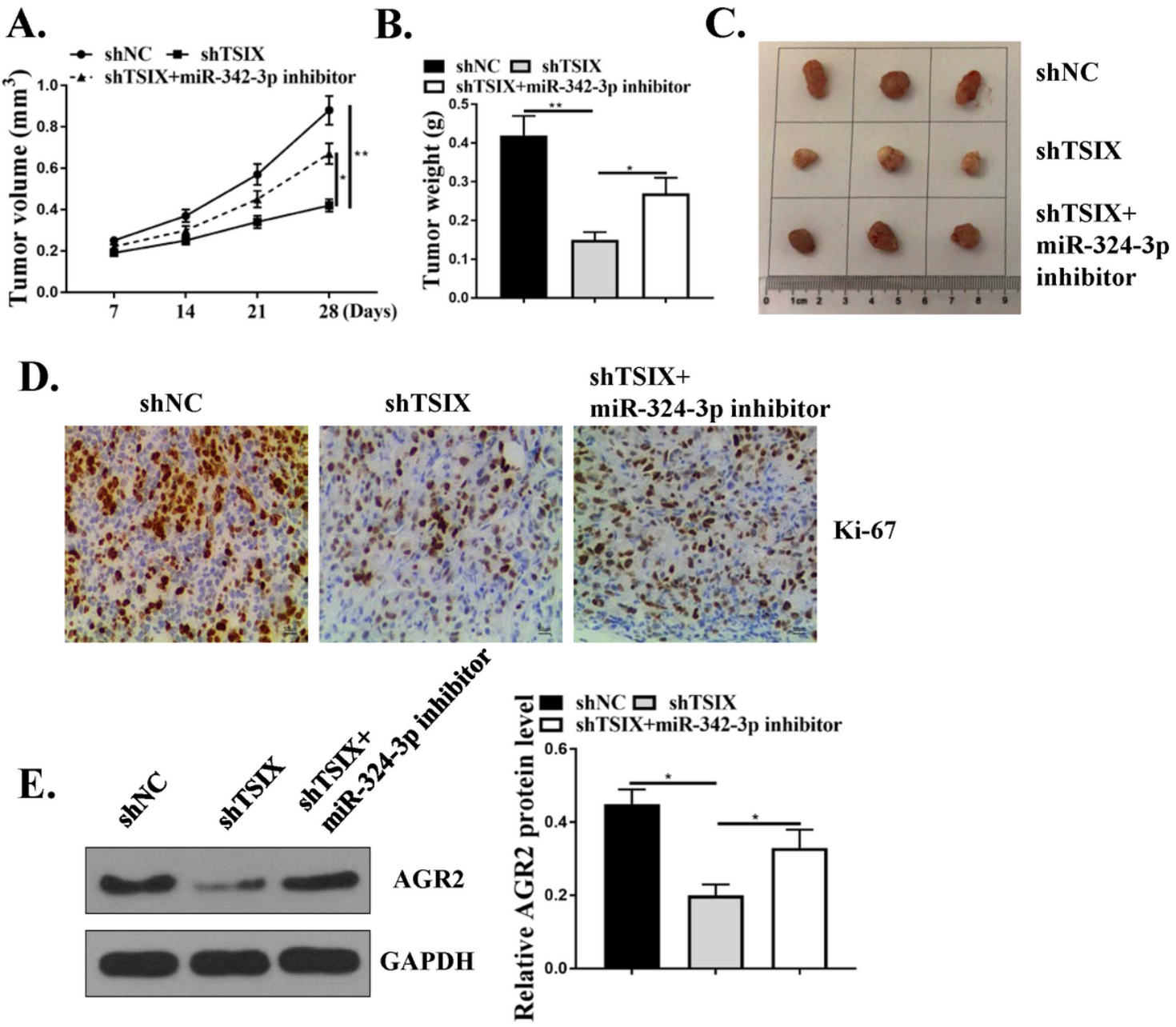

Figure 6

Downregulation of TSIX inhibited tumor development in vivo through targeting miR-342-3p/AGR2 axis. (A) Tumor volume of xenograft mice was evaluated every 7 days for 28 days. (B) Tumor weight of xenograft mice was evaluated at day 28. (C) The representative images of xenograft tumor from different

groups. (D) Cell proliferation in tumor tissues was evaluated by Ki-67 staining assay. × 200 magnification, scale bar = 100 μm. (E) The protein expression of AGR2 in tumor tissues from different groups was evaluated by western blot. Full-length blots/gels are presented in Supplementary Figure 5. N = 6, * $p < 0.05$.

Supplementary Files

This is a list of supplementary files associated with this preprint. Click to download.

- Supplementarydata.docx
- AuthorChecklistFull.pdf